Continuous Monitoring of P_i Release Following Nucleotide Hydrolysis in Actin or Tubulin Assembly Using 2-Amino-6-mercapto-7-methylpurine Ribonucleoside and Purine-Nucleoside Phosphorylase as an Enzyme-Linked Assay†

Ronald Melki, Stéphane Fievez, and Marie-France Carlier*

Laboratoire d'Enzymologie et Biochimie Structurales, Centre National de la Recherche Scientifique, 91198 Gif-Sur-Yvette, France

Received June 4, 1996; Revised Manuscript Received July 15, 1996⊗

ABSTRACT: ATP and GTP are hydrolyzed during self-assembly of actin and tubulin, respectively. It is known that nucleotide is hydrolyzed on the polymer in two consecutive steps, chemical cleavage of the γ-phosphate followed by the slower release of P_i. This last step has been shown to play a crucial role in the dynamics of actin filaments and microtubules. Thus far, evidence for a transient GDP−P_i state in microtubule assembly has been obtained using a glass fiber filter assay that had a poor time resolution [Melki, R., Carlier, M.-F., & Pantaloni, D. (1990) *Biochemistry 29*, 8921−8932]. We have used a new P_i assay [Webb, M. R. (1992) *Proc. Natl. Acad. Sci. U.S.A. 89*, 4884−4887], in which the purine phosphorylase catalyzes the phosphorolysis of 2-amino-6-mercapto-7-methylpurine ribonucleoside (MESG) into mercaptopurine and ribose phosphate, which is accompanied by an increase in absorbance. This enzyme-linked assay has been used to follow the release of P_i during polymerization of Mg−actin. A value of 350 s was found for the half-time for P_i release on F-actin, in good agreement with previous determinations. The release of P_i following GTP hydrolysis in microtubule assembly was followed using a stopped-flow apparatus. Rapid microtubule assembly was achieved using taxol. The use of a stopped-flow apparatus permitted the continuous recording, with a dead time of 0.8 ms, of both time courses of microtubule assembly and P_i release with greatly improved time resolution. The release of P_i developed with a short lag (35 and 2 s for G-actin and tubulin, respectively) following assembly and appeared 50-fold faster on microtubules than on actin filaments.

Actin filaments and microtubules are dynamic polymers which play a crucial role in cell motility. Actin and tubulin bind nucleotide (ATP and GTP, respectively) which is irreversibly hydrolyzed during the self-assembly process. Nucleotide hydrolysis takes place on the polymerized subunits following their endwise association to the growing polymers, in two consecutive steps: chemical cleavage of the γ-phosphate followed by release of P_i in the medium [Carlier & Pantaloni, 1981; reviewed in Carlier (1989)]. It has been shown that phosphate release, rather than chemical cleavage of the γ-phosphoester bond, plays a crucial role in the control of the dynamics of actin filaments (Carlier & Pantaloni, 1988) and microtubules (Carlier *et al.*, 1988, 1991). This reaction is associated with the weakening of protein-protein interactions in the polymer, i.e. XDP subunits dissociate much faster from polymer ends than XDP−P_i subunits. In microtubules, P_i release is linked to the transition of the assembled tubulin subunits from a "straight" conformation to a "curved" conformation (Melki *et al.*, 1989) and is accompanied by a large decrease in microtubule rigidity[1] (Venier *et al.*, 1994) and a tendency of protofilaments to curl as the lateral bonds between adjacent protofilaments are weakened. Recent structural data (Hyman *et al.*, 1995) have brought confirmation of the straight−curved conformational transition linked to GTP hydrolysis. Therefore, the existence of a more rigid "cap" of GDP−P_i tubulin subunits at the ends of microtubules prevents the rapid depolymerization of the GDP core. The fact that the resulting dynamic instability behavior (Hill & Carlier, 1983; Carlier *et al.*, 1984, 1987; Mitchison & Kirschner, 1984; Hill, 1985, 1987; Horio & Hotani, 1986; Walker *et al.*, 1988), which plays an important role in microtubule function, seems to be finely regulated through the cell cycle has prompted a large number of experiments aimed at understanding how the size and geometry of the cap correlated with the dynamic properties of a given microtubule. To resolve this issue, it is necessary to know by which mechanism and at which rate P_i is released from assembled GDP−P_i tubulin subunits.

Previous kinetic analysis of the correlation between the initial rates of polymer growth and nucleotide hydrolysis indicated that the nucleotide was hydrolyzed in a "vectorial" fashion, essentially at the XTP−XDP boundary, and that the size of the cap was limited by the creation of new boundaries within long stretches of XTP subunits (Carlier & Pantaloni, 1986; Carlier *et al.*, 1987; Melki *et al.*, 1990; Burns, 1991).

† This work was supported by the Centre National de la Recherche Scientifique, the Association pour le Recherche sur le Cancer, the Ligue Nationale Française contre le Cancer, and the Association Française contre les Myopathies.

* To whom correspondence should be adressed. Telephone: 33 1 69 82 34 65. Fax: 33 1 69 82 31 29. E-mail: carlier@lebs.cnrs-gif.fr.

⊗ Abstract published in *Advance ACS Abstracts,* August 15, 1996.

[1] A recent contrary view was expressed (Caplow *et al.*, 1994); however, this conclusion is incorrect due to a sign error in the calculation of the free energy changes linked to the different steps of GTP hydrolysis on microtubules. The free energy ΔG_1 linked to the cleavage of the γ-phosphate of GTP is equal to the free energy for the overall hydrolysis reaction (−0.9 kcal/mol) *minus* (and not *plus* as used by Caplow *et al.*) the free energy for P_i dissociation (+2.18 kcal/mol). Therefore, ΔG_1 is largely negative and not positive.

S0006-2960(96)01325-6 CCC: $12.00

These studies also showed that the cap was very small at steady state; the same conclusion was reached in a recent work where the cap size was visualized using fluorescently labeled tubulin (Drechsel & Kirschner, 1994). Other works failed to detect any GTP cap and proposed that GTP hydrolysis was tightly coupled to microtubule growth. Overall, the difficulty of the problem of the coupling between GTP hydrolysis and microtubule assembly appears in the many conflicting reports from different laboratories, some in support of the GTP caps (Caplow *et al.*, 1988), some others in support of a tightly coupled GTP hydrolysis and absence of the GTP cap (Caplow, 1986; O'Brien *et al.*, 1987; Stewart *et al.*, 1990).

As discussed earlier (Melki *et al.*, 1990), two requirements must be fulfilled in order to have a chance to observe long stretches of GTP and/or GDP−P_i subunits on microtubules. (1) The rate of microtubule assembly must be larger than that of GTP hydrolysis and subsequent P_i release, and (2) the amount of P_i released in the medium must be very quickly and accurately measured. The first condition was reached using taxol to induce rapid tubulin assembly into microtubules. Thus far, evidence for a transient GDP−P_i state in microtubule assembly has been provided using a glass fiber filter assay which has a poor time resolution (∼2 s) and moderate accuracy, with time intervals of 10−20 s between each point. The recently developed (Webb, 1992) enzyme-linked spectroscopic assay allowing continuous monitoring of P_i release was found to be a more efficient method for following the kinetics of free P_i in solution during microtubule assembly. In addition, both the short dead time of the stopped-flow instrument and the accurate definition of the time zero in kinetic curves provide a reliable kinetic analysis of P_i release during microtubule assembly.

MATERIALS AND METHODS

Chemicals. GTP and DTT were purchased from Boehringer Mannheim. MES was from Calbiochem, and 2-amino-6-chloropurine ribonucleoside, EGTA, and PIPES came from Sigma. Taxol was a gift from D. Guénard, and MESG was synthesized and purified as described (Broom & Robins, 1964). All other chemicals were Merck's analytical grade. Calf spleen purine-nucleoside phosphorylase (EC 2.4.2.1) was purchased from Sigma.

Actin and Tubulin. Actin was purified from rabbit muscle acetone powder (Spudich & Watt, 1971; Eisenberg & Kielley, 1974) and isolated as Ca-ATP−G-actin by Sephadex G200 chromatography (McLean-Fletcher & Pollard, 1980) in G buffer [5 mM Tris-HCl (pH 7.8), 0.2 mM DTT, 0.1 mM $CaCl_2$, 0.2 mM ATP, and 0.01% NaN_3]. The 1:1 complex Ca-ATP−G-actin without free ATP was prepared by treatment of Ca-ATP−G-actin solution with Dowex 1x8 equilibrated in ATP-free G buffer (G_o buffer). Conversion of Ca−G-actin into Mg−G-actin was achieved prior to polymerization by a 3 min preincubation in the presence of 0.2 mM EGTA and $MgCl_2$ at a concentration of 1 molar equiv to actin plus a 10 μM excess.

Pure tubulin was prepared from fresh pig brain by three assembly−disassembly cycles (Shelanski *et al.*, 1973) followed by phosphocellulose (Whatman P11) chromatography (Weingarten *et al.*, 1975). Tubulin was stored at −80 °C in MG buffer [0.05 M MES (pH 6.8), 0.5 mM EGTA, 0.25 mM $MgCl_2$, 4 M glycerol, and 1 mM GTP]. The 1:1 GTP−tubulin complex was isolated free of unbound nucleotide by loading 1 mL of the tubulin stock solution on a Pharmacia PD-10 Sephadex G-25 column (9.1 mL bed) pre-equilibrated in P buffer [100 mM PIPES (pH 6.9), 1 mM EGTA, and 3 mM $MgCl_2$]. Elution of the column was carried out at 4 °C with the equilibrating buffer. The protein concentration in each collected fraction (0.4 mL) was determined from wavelength scans (240−320 nm). Tubulin eluted from this column in six fractions (V_e = 3.6−6mL). Only the first four fractions were pooled, to avoid contamination by free nucleotide. When 1 mL of a 1 mM GTP solution in P buffer was loaded onto the column, the presence of 5 μM GTP was detected in the fraction eluting between 6.8 and 7.2 mL, the majority of GTP eluting in the subsequent fractions. These data demonstrate that no free GTP was contaminating the 1:1 GTP−tubulin complex in our experiments. The 1:1 [γ ^{32}P]GTP−tubulin complex was prepared using the same procedure following incubation of tubulin at 0 °C for 1 h in the presence of 1 mM [γ ^{32}P]GTP (50 Ci/mol).

Table 1: Identification of Nucleotides Bound to Tubulin in Four Different Preparations of 1:1 GTP−Tubulin Complex[a]

	total nucleotide bound to tubulin	
preparation	% GTP	% GDP
1	95.35	4.65
2	100	0
3	98.8	1.2
4	100	0

[a] The 1:1 GTP−tubulin complex (20 μM) was prepared, and perchloric acid extractions were performed as described in Materials and Methods. UV spectrophotometric measurements showed that the concentration of guanine nucleotides in the extracts corresponded to 2.1 ± 0.1 GXP per tubulin. 2.0 nmol of nucleotide was injected onto the Synchropack AX300 HPLC column. The percentages of GDP and GTP present in the extracts were derived from measurements of the areas under the peaks of GDP and GTP.

The nucleotide content of the 1:1 tubulin-GTP complex was assessed by HPLC anion exchange chromatography of the perchloric extract using a Synchropack AX300 column (Synchrom, Inc.) and isocratic elution by 0.35 M KH_2PO_4 buffer (pH 3.5), containing 1.3 M NaCl. As summarized in Table 1, and consistent with previous data from our laboratory (Melki *et al.*, 1990; Melki & Carlier, 1993), 95.5−100% of the bound nucleotide was GTP-indicating that at most 9% of the tubulin had GDP at the E-site.

The concentrations of the 1:1 ATP−actin and GTP−tubulin complexes were determined spectrophotometrically using an extinction coefficient of 0.617 mg^{-1} cm^2 at 290 nm and a molecular mass of 42 kDa for actin (Gordon *et al.*, 1976) and an extinction coefficient of 1.2 mg^{-1} at 277 nm (Detrich *et al.*, 1978) and a molecular mass of 100 kDa (Krauhs *et al.*, 1981) for tubulin.

Calf spleen purine-nucleoside phosphorylase was extensively dialyzed prior to the experiment against either G_o or P buffer.

Measurements of Actin or Tubulin Self-Assembly and of P_i Release. In the presence of MESG and purine-nucleoside phosphorylase, the release of P_i accompanying self-assembly of actin or tubulin leads to an increase in absorbance at 360 nm. The assembly of microtubules and actin filaments also causes an increase in turbidity, i.e. in absorbance of the solution at 360 nm. Hence, in the presence of MESG and phosphorylase, the sum of both reactions is monitored by

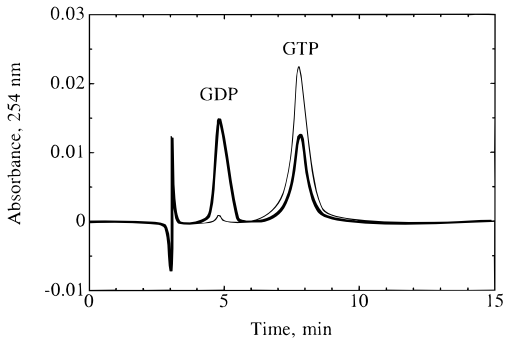

FIGURE 1: Nature of the nucleotide bound to tubulin before assembly and 30 s after taxol-induced assembly of microtubules. The 1:1 GTP−tubulin complex (20 μM) was assembled into microtubules at 25 °C in the presence of taxol (40 μM). Assembly reaction was arrested 30 s after addition of taxol by immediate transfer of 100 μL of the microtubule solution into an ice-cold tube containing 12 μL of 40% $HClO_4$. A sample of the 1:1 GTP−tubulin complex solution prior to addition of taxol was treated in the same way. The pH of the solutions was brought to 4.0 by addition of 0.4 M sodium acetate, and the extracts were clarified by centrifugation at 15000*g* and 4 °C for 5 min. UV spectrophotometric measurements showed that the concentration of guanine nucleotides in the extracts corresponded to 2.1 ± 0.1 GXP per tubulin. Three nanomoles of nucleotide was injected onto the HPLC column under the conditions described in Materials and Methods. The percentages of GDP and GTP present in the extracts were derived from measurements of the areas under the peaks of GDP and GTP in HPLC patterns obtained before (thin line) and after assembly of microtubules (solid line).

the overall absorbance change at 360 nm. In the presence of either MESG alone or phosphorylase alone, only the self-assembly reaction was monitored. Two control assays were first run to verify that the time course of spontaneous assembly was not altered by either MESG or phosphorylase. The time course of self-assembly recorded in the presence of either MESG alone or enzyme alone was then subtracted from the overall kinetic curve to yield the time course of P_i release. Experiments were conducted as follows.

Actin assembly and P_i release were monitored in a Cary 1 spectrophotometer following addition of 0.1 M KCl and 1 mM $MgCl_2$ to 1:1 Mg-ATP−G-actin complex (30 μM, 1 mL) in G_o buffer containing 80 μM MESG and 5 units/mL phosphorylase.

Tubulin assembly and P_i release were monitored at 360 nm in the stopped-flow apparatus (DX.17 MV, Applied Photophysics) at temperatures of 20, 25, or 37 °C (±0.5 °C). The optical path was 1 cm, and the slits of the monochromator were 1 mm (4 nm bandwidth). One of the drive syringes contained 1:1 GTP−tubulin complex (20−40 μM) together with MESG (200 μM) and phosphorylase (30−60 units/mL) in buffer P. The other drive syringe contained taxol (2 molar equiv per tubulin, i.e. 40−80 μM) also in buffer P. Light scattering measurements made at 280 nm checked that in buffer P and at 20 °C the solubility of taxol was 76 μM. Therefore, at the highest taxol concentration used (80 μM), 95% of the taxol was soluble before 2-fold dilution upon mixing. The presence of MESG and enzyme together with GTP−tubulin before polymerization was started helped to eliminate any putative trace of P_i contaminating the solution of GTP−tubulin.

The nature of nucleotide bound to microtubules rapidly assembled with taxol as described above was determined by HPLC of the perchloric extract carried out 30 s after polymerization was started. Figure 1 shows the HPLC patterns obtained before and after assembly of microtubules, which clearly indicate that (1) only GTP was bound to tubulin before polymerization and (2) 50% of the bound GTP (presumably E-site-bound) had been hydrolyzed into GDP 30 s after polymerization in the presence of taxol. Finally, a correlation was established between the amount of released P_i derived from the absorbance change in the MESG−phosphorylase assay and the amount of hydrolyzed ATP derived from the acid labile phosphate measurement. Tubulin was equilibrated in the presence of γ-^{32}P-labeled GTP. The 1:1 [γ-^{32}P]GTP−tubulin complex was isolated by Sephadex G-25 chromatography as described above and assembled at 40 μM in the presence of 80 μM taxol. The reaction was quenched in ammonium molybdate−1 N HCl at time 30 s, and ^{32}P was extracted as described (Carlier & Pantaloni, 1981; Carlier *et al.*, 1987). Thirty-nine and forty micromolar P_i were found in two independent measurements, which showed that 97% at least of the 1:1 GTP−tubulin complex had hydrolyzed the E-site-bound GTP 30 s after the onset of assembly.

Electron Microscopy. Microtubules assembled from the 1:1 GTP−tubulin complex (17 μM) in the presence of 2 molar equiv of taxol at 20 °C were rapidly adsorbed onto a grid 5 s after the onset of polymerization and negatively stained with 1% uranyl acetate 10 s later. Electron micrographs of different fields of the preparation (magnification of 35000×) were analyzed using Optimas image analysis software to obtain the length distribution of rapidly assembled polymers. The lengths of both closed microtubules and open short microtubular sheets (representing about 30% of the total polymers) were computed without distinction.

Data Analysis and Simulation. The kinetics of actin or tubulin polymerization, ATP or GTP hydrolysis, and P_i release were analyzed within the following simplified scheme:

Scheme 1

$$M_T \xrightarrow{k_1} P_T \xrightarrow{k_2} P_D P_i \xrightarrow{k_3} P_D + P_i$$

where M_T represents a monomer (G-actin or $\alpha\beta$-tubulin) with NTP bound and P_T, $P_D P_i$, and P_D represent the different states of NTP hydrolysis on the polymer. The processes of polymerization, chemical cleavage of NTP, and P_i release are assumed to be irreversible first-order reactions of rate constants k_1, k_2, and k_3, respectively. Hence, k_1 actually represents k_+[P], where k_+ is the bimolecular rate constant for association of a monomer M_T to a polymer end and [P] the concentration of elongating polymer ends. The assumption that the polymerization step is quasi-irreversible is validated by the fact that, under the experimental conditions used here, the critical concentrations (for assembly of both actin and tubulin in the presence of taxol) are at least 1 order of magnitude lower than the total concentration of monomers so that the reverse reaction (dissociation of subunits from polymer ends) can be neglected, within less than 10% error, over 90% of the polymerization process.

This scheme is simplified in the sense that the nucleation step is not accounted for, and only the growth process onto preformed nuclei is described by the pseudo-first-order rate constant k_1. The second simplification is that k_2 and k_3 are assumed to represent rate constants for random nucleotide hydrolysis and phosphate release on any T− or D−P_i-bound

subunit of the polymer. At least, in the case of chemical cleavage of the γ-phosphate, evidence for a cooperatively enhanced rate of hydrolysis on subunits at the T−DP_i boundary has been obtained for microtubules (Melki *et al.*, 1990) and actin (Carlier, 1987); however, a different view (Ohm & Wegner, 1994) was recently expressed. Therefore, the physical significance of k_2 and k_3 should be understood within the restriction of a random mechanism for ATP hydrolysis and P_i release.

RESULTS AND DISCUSSION

Optimization of an Enzyme-Linked Assay for Continuous Monitoring of P_i Release during Assembly of Actin Filaments and Microtubules. In a previous work (Carlier, 1987), an enzyme-linked assay consisting of glyceraldehyde-3-phosphate dehydrogenase and phosphoglycerate kinase, initially designed by Trentham *et al.* (1972), allowed the continuous monitoring of P_i release following hydrolysis of ATP in F-actin assembly. This assay unfortunately works adequately only at pH $\geq$7.5; hence, it could not be used in microtubule assembly which requires pH $\leq$7.1. The novel and sensitive P_i assay (K_M of P_i = 26 μM; K_M of MESG = 70 μM and k_{cat} = 40 s^{-1} at 25 °C) developed by Webb (1992) uses the change in absorbance at 360 nm linked to the conversion of 2-amino-6-mercapto-7-methylpurine ribonucleoside (MESG) into mercaptopurine and ribose phosphate catalyzed by purine-nucleoside phosphorylase. Although the absorbance change which is due to a difference in the pK_as of the MESG substrate and the product mercaptopurine is maximum at pH 7.6 ($\Delta\epsilon$ = 10 000 M^{-1} cm^{-1} at 20 °C), the assay can work at a lower pH (e.g. 6.9) at which tubulin can polymerize, pending a lower molar differential extinction coefficient. Figure 2A shows that in buffer P (pH 6.9) a linear absorbance change was observed upon increasing the P_i concentration up to 50 μM. The molar absorbance change was slightly dependent on temperature (Figure 2A, inset) and varied between 5940 M^{-1} cm^{-1} ($\pm$50 M^{-1} cm^{-1}) at 12 °C and 4700 M^{-1} cm^{-1} ($\pm$50 M^{-1}.cm^{-1}) at 30 °C. Figure 2B shows that, using 10 units/mL phosphorylase, 70% of the added 40 μM P_i was consumed in P buffer in less than 3 s. Lower amounts of P_i were totally consumed within a shorter period of time.

P_i Release in Assembly of ATP−Actin. The efficiency of the MESG−phosphorylase assay was first examined in monitoring P_i release following ATP hydrolysis during actin self-assembly. Figure 3A shows that the turbidity increase at 360 nm associated with actin polymerization alone (i.e. in the presence of either MESG or enzyme) was very small, typically 0.001 cm^{-1} per absorbance unit per micromolar assembled actin (inset). The absorbance change due to titration of P_i was much larger, 0.010 absorbance units per micromolar P_i; therefore, the release of P_i represented the essential portion of the overall absorbance change when actin was assembled in the presence of both MESG and enzyme. After subtraction of the absorbance change due to actin assembly alone from the overall kinetic curve, the time course of P_i release was obtained (see Materials and Methods). One equivalent of P_i was titrated per F-actin at the end of the reaction. The normalized time courses of actin assembly and P_i release are shown in Figure 3B. While actin assembly was completed in less than 2 min, P_i release was much slower ($t_{1/2} \sim$ 6 min) and exhibited a lag time of 0.6 min, indicating that it took place on F-actin following the incorporation of actin in the filament. The difference

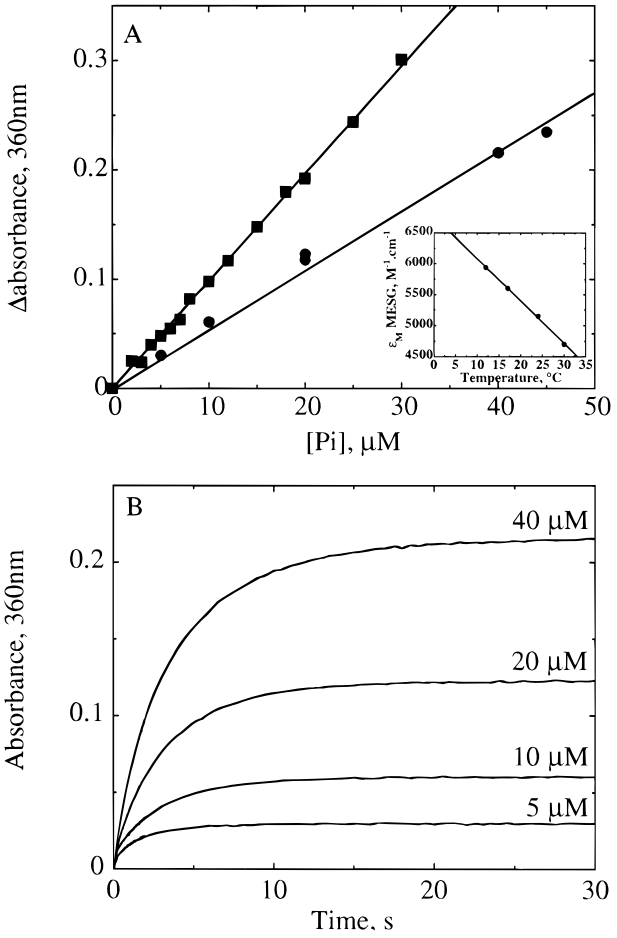

FIGURE 2: Change in absorbance at 360 nm due to the phosphorolysis of MESG as a function of P_i concentration. (A) Absorbance titration curves of P_i at 20 °C by the phosphorylase/MESG coupled system. Assay conditions were either 5 mM Tris-HCl (pH 7.8), 0.2 mM DTT, 0.1 mM $CaCl_2$, 0.01% NaN_3, 100 μM MESG, and 10 u/mL phosphorylase (■) or 0.1 M PIPES (pH 6.9), 3 mM $MgCl_2$, 0.5 mM EGTA, 100 μM MESG, and 10 u/mL phosphorylase (●). Aliquots of a potassium phosphate solution at the same pH were added to the desired concentration, and the absorbance was monitored at 360 nm. The inset represents the temperature dependence of the change in molar absorbance in P buffer. (B) Rapid kinetics of P_i titration by the phosphorylase/MESG coupled system in P buffer. Potassium phosphate at the indicated concentration in 0.1 M PIPES buffer (pH 6.9), 1 mM $MgCl_2$, and 0.5 mM EGTA was mixed at 20 °C with 100 μM MESG and 10 u/mL phosphorylase in the same buffer, and the absorbance at 360 nm was recorded.

between the time courses of actin assembly and P_i release represents the time dependence of the sum of the first two kinetic intermediates in filament assembly, F-ATP and F-ADP−P_i.

The results are in agreement with data previously published (Carlier & Pantaloni, 1986; Carlier, 1987) and validate the use of the MESG−phosphorylase assay as an enzyme linked assay to monitor ATP hydrolysis associated with actin polymerization.

P_i Release during Taxol-Induced Rapid Assembly of Microtubules. As explained earlier (Melki *et al.*, 1990), to obtain the most accurate information about the kinetics of P_i release, conditions under which tubulin assembles very rapidly are necessary. We indeed already know that, in a range of relatively slow rates of polymerization, P_i release seems to occur concomitantly with microtubule growth; hence, the rate constant for P_i dissociation cannot be

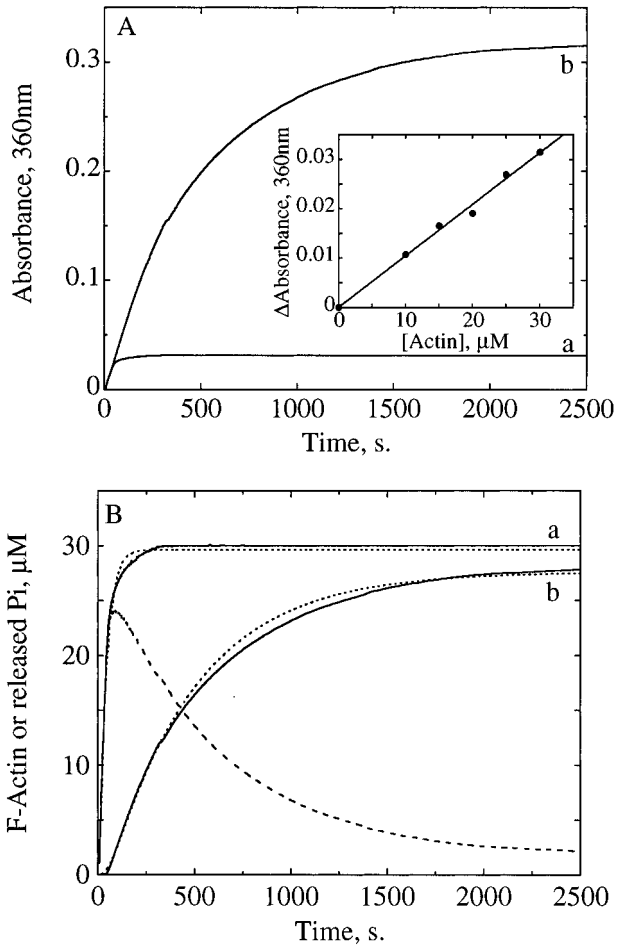

FIGURE 3: Kinetic analysis of the elementary steps in ATP hydrolysis on actin filaments. (A) The time course of actin polymerization and phosphate release from Mg−F-actin was monitored by absorbance at 360 nm using a spectrophotometer that was thermostated at 20 °C (light path of 1 cm). Experiments were carried out in Go buffer [5 mM Tris-HCl (pH 7.8), 0.1 mM $CaCl_2$, 0.1 mM DTT, and 0.01% NaN_3]. Conversion of Ca-ATP−G-actin to Mg-ATP−G-actin was achieved by a 3 min preincubation in the presence of 40 μM $MgCl_2$ and 200 μM EGTA. The polymerization of 1:1 Mg-ATP−G-actin complex (30 μM) was initiated by addition of 0.1 M KCl and 1 mM $MgCl_2$ to the G-actin solution supplemented with 80 μM MESG in the absence (trace a) or presence (trace b) of 10 u/mL purine-nucleoside phosphorylase. The inset represents the linearity of absorbance at 360 nm as a function of F-actin concentration. (B) Evolution with time of the different kinetic intermediates in actin polymerization. Curve a represents the molar amount of polymerized actin (F-actin) derived from the turbidity data (trace a in panel A). Curve b represents the molar amount of polymerized F-actin−ADP (F-ADP) derived from the P_i release kinetics (difference between traces b and a in panel A). The difference between the polymerization curve and the curve of P_i release is displayed in dashed lines and represents the evolution with time of F-ATP and F-ADP−P_i intermediates. Theoretical time courses of actin assembly and P_i release were simulated with the proposed model using the KINSIM software and are shown in dotted lines. Values of the rate constants adjusted to obtain the best fit of simulated kinetic curves to the experimental data are given in Table 2.

determined under such conditions. The 1:1 GTP−tubulin complex was therefore rapidly assembled in microtubules in the stopped-flow apparatus using taxol. Control experiments first showed that neither MESG nor phosphorylase by itself affected the kinetics of turbidity change associated with microtubule assembly. Sedimentation assays showed that at most 0.3−0.4 μM tubulin was not assembled at the end of the reaction; i.e. 97.6−98.2% of the tubulin was polymerized with a molar excess of taxol in order to ensure a quicker binding of taxol to tubulin, particularly at the end of the tubulin assembly reaction. At 25 °C, the rapid mixing of tubulin (17 μM) with taxol (34 μM) yielded a sigmoidal polymerization curve at 360 nm, exhibiting a short lag of 0.8 s due to nucleation, followed by a rapid increase in turbidity as shown in Figure 4A (curve a). In the presence of both MESG and phosphorylase, the absorbance change was larger (curve b). Increasing the concentration of phosphorylase by 2-fold yielded a curve that could be superimposed on curve b. Therefore, phosphorylase was not kinetically limiting the time course of P_i detection. If the release of P_i was tightly coupled to tubulin polymerization, the absorbance change in the presence of the enzyme-linked system would be simply homothetic to the absorbance change recorded in the absence of enzyme.[2] The calculated curve for a tightly coupled mechanism is drawn (dashed line) in Figure 4A and appears to be incompatible with the experimental trace (solid lines). The expanded view of the early time points (0−5 s) of the reactions shown in the inset confirms that the signal to noise ratio and time resolution of the data are high enough to exclude a tight-coupling mechanism for GTP−tubulin polymerization and P_i release and favor a model in which P_i release occurs with a delay following tubulin polymerization. The difference between curves b and a represented the absorbance change due to P_i release. The data were plotted in terms of molar amounts of assembled tubulin and released P_i using a specific molar turbidity change of 0.0183 ± 0.0018 cm^{-1} per micromolar assembled tubulin and 0.00505 cm^{-1} μM^{-1} for P_i (Figure 4B). The resulting time courses are shown in Figure 4C. Comparison of the time course of tubulin polymerization (curve a) and of P_i release (curve b) demonstrates that P_i release occurs with a delay of 2 s following the onset of assembly and develops on assembled microtubules with a half-time of 10 s. The same curves a and b were obtained at different tubulin concentrations. The specific turbidity of assembled tubulin shows some fluctuation from one experiment to the other (Figure 4B); however, within a single given experiment, corresponding to e.g. curves a and b in Figure 4A, the fluctuations are 1 order of magnitude lower and the recordings coming from consecutive shots in the stopped flow were highly superimposable. These data show that if the assembly process was slower (e.g. with a $t_{1/2}$ of ≥10 s) it would be much more difficult to appreciate the intrinsic rate of P_i release and the kinetic uncoupling of the different steps.

At time 60 s, the amount of released P_i was 14.6 μM while 16.6 μM tubulin had polymerized according to the absorbance measurements. The uncertainty on P_i concentration is less than 2%, given the accuracy in the determination of the molar extinction coefficient (Figure 2A, inset). Hence, at most 14.9 μM P_i might have been released after 1 min. The fact that the molar ratio of released P_i to assembled tubulin is 0.86 instead of 1.00 is unlikely to indicate that

[2] The calculated dashed line was derived from curve a using an extinction coefficient of 0.0183 and assuming that the turbidity change in curve a was proportional to the mass amount of polymerized tubulin at all times of the assembly process. As noted in the Results and Discussion, the relative turbidity change is probably lower in the early steps than in the late assembly steps; hence, the calculated dashed curve shown in Figure 4A is probably below the more realistic theoretical curve that would be expected within a tight-coupling mechanism.

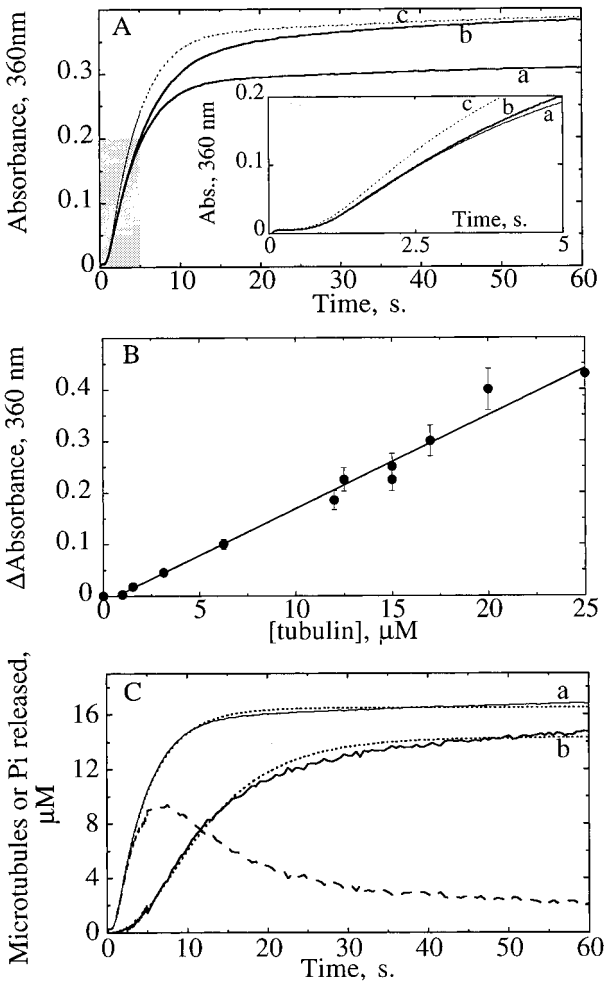

FIGURE 4: Kinetic analysis of the elementary steps in GTP hydrolysis on microtubules. (A) The time course of tubulin polymerization and phosphate release from microtubules was monitored by absorbance using a stopped-flow spectrophotometer (DX.17 MV, Applied Photophysics) thermostated at 25 °C (optical path length of 1 cm). The experiment was conducted as described in Materials and Methods, with final concentrations of tubulin and taxol of 17 and 34 μM, respectively, in the absence (trace a) or presence (trace b) of 27 u/mL purine-nucleoside phosphorylase. Trace c (dotted line) represents the calculated curve for a mechanism in which GTP hydrolysis is tightly coupled with assembly. The turbidity data recorded during the first 5 s of tubulin assembly in the absence (a) or presence (b) of purine-nucleoside phosphorylase are expanded in the inset. Curves a and b are superimposable in the early steps of assembly and diverge 2 s following the onset of assembly. Also note that the calculated time course assuming tight coupling (curve c, dashed) is significantly different from the experimental trace b. (B) Extent of the change in absorbance at 360 nm as a function of the concentration of polymerized tubulin. The 1:1 GTP−tubulin complex, in P buffer, at the concentrations indicated, was assembled in the stopped flow in the presence of 2 molar equiv of taxol. The extent of absorbance change at 360 nm, 1 cm optical path length, was recorded at 25 °C. (C)The evolution with time of the different kinetic intermediates in microtubule assembly. Curve a represents the molar amount of assembled tubulin (MT) derived from the turbidity data (trace a in panel A). Curve b represents the molar amount of assembled GDP−tubulin (MT-GDP) derived from the P_i release kinetics (difference between traces b and a in panel A). The difference between the polymerization curve (a) and the curve of P_i release (b) represents the evolution with time of GTP microtubules and GDP−P_i microtubules (dashed line). Time courses of assembly and P_i release were simulated with the proposed model using the KINSIM software (dotted lines). Values of rate constants adjusted to obtain the best fit of simulated kinetic curves to the experimental stopped-flow traces are given in Table 2.

14% of the GTP initially bound remains unhydrolyzed on microtubules. Indeed, using γ-^{32}P-labeled GTP−tubulin (40 μM), we found that 97% of the 40 μM bound GTP was transformed into acid-labile $^{32}P_i$ after 2 min, and less than 2% of the ^{32}P radioactivity remained bound to microtubules sedimented after 2 min. The slight discrepancy between the amounts of polymerized tubulin and released P_i may be explained by the microheterogeneity of tubulin. P_i might be released more slowly (i.e. within 2−3 min) on a small percentage of the population of assembled tubulin, as was earlier noticed in the assembly of microtubules from Cr-GTP−tubulin (Carlier *et al.*, 1991). Alternatively, defects in the microtubule lattice leading to a slow hydrolysis of GTP on microtubules may account for the little descrepancy between the amounts of assembled tubulin and released P_i. The main conclusion that P_i release is not tightly coupled to tubulin polymerization however is not affected by the small difference between the measured values of assembled tubulin and released P_i.

Analysis of the Data. Data were analyzed within Scheme 1 (see Materials and Methods). The data summarized in Table 2 show that, when the rate of tubulin polymerization was higher, the rates of GTP hydrolysis and P_i release were higher. The fact that the values of k_2 and k_3 increased when the number of microtubules increased supports a vectorial mechanism for both cleavage of GTP and release of P_i. Since the same amount of phosphorylase was used in the above experiments, the result is also a confirmation that the apparent slow release of P_i is not an artifact resulting from the kinetically limiting catalysis of MESG phosphorolysis by the enzyme; in the latter case, the value of k_3 would have been independent of the rate of microtubule assembly but dependent on the concentration of enzyme, in contrast to the evidence presented here.

A good fit of the kinetic data for P_i release required that the NTP cleavage step (k_2) be included in the kinetic scheme. In other words, the lag observed in P_i release was such that, if k_2 was very large ($k_2 \gg 0.1$ s^{-1}), no satisfactory value for k_3 could be found that could accommodate the whole experimental curve. For actin assembly, values of 0.035 and 0.003 s^{-1} were found for k_2 and k_3, respectively. In reasonable agreement, values of 0.005−0.006 s^{-1} had previously been found for k_3 using NBD-labeled actin (Carlier & Pantaloni, 1986; Carlier, 1987). The rates of GTP cleavage and P_i release in microtubule assembly were both faster than in the actin system, in agreement with previous data using the glass fiber filter assay (Melki *et al.*, 1990). The rates of tubulin assembly that could be monitored with accuracy using the stopped flow were about 5-fold higher than in our previous work, due to the larger amount of taxol used in the present experiments. The affinity of taxol for dimeric tubulin is in the 10^5 M^{-1} range (Carlier & Pantaloni, 1983), i.e. much lower than for assembled tubulin. Hence, nucleation is enhanced by addition of a large excess of taxol compared to the tubulin concentration. On the other hand, the 2−3-fold difference in the values of k_3 (P_i release) found here and in our previous work using a glass filter assay (Melki *et al.*, 1989) cannot be solely due to the difference in time resolution provided by the two techniques. A tentative explanation may be proposed, on the basis of the difference in chemical perturbation of reversible reactions introduced by the two techniques. The filter assay rapidly separates microtubules from the solution without changing

Table 2: Rate Parameters for Polymerization, Hydrolysis, and Release from F-Actin or Microtubules

	concentration (μM)	temperature (°C)	k_1 (s^{-1})	k_2 (s^{-1})	k_3 (s^{-1})
actin	30	20	0.032 ± 0.007	0.035 ± 0.005	0.0026 ± 0.0004
tubulin	12	25	0.3	0.3	0.15
	15	20	0.25	0.25	0.12
	17	25	0.35	0.35	0.11
	20	15	0.2	0.1	0.05
	30[a]	37[a]	0.050 ± 0.002[a]	0.065 ± 0.007[a]	0.02 ± 0.002[a]

[a] Pseudo-first-order rate of polymerization (k_1), first-order rate of GTP hydrolysis (k_2), and first-order rate of P_i liberation (k_3) values used to fit theoretical curves to experimental data obtained upon the assembly of 1:1 GTP−tubulin complex in the presence of 1.5 molar equiv of taxol by Melki *et al.* (1990). [b] The rate parameters refer to the scheme given in the text.

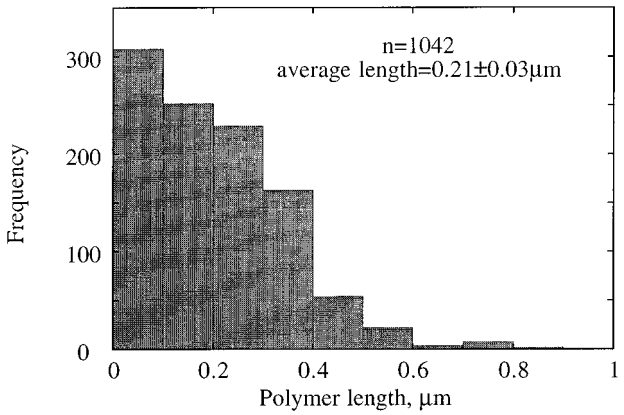

FIGURE 5: Histogram of the length distribution of microtubular polymers formed at $t = 15$ s of taxol-induced polymerization of 1:1 GTP−tubulin complex. The length of 1042 short microtubules and flat sheets assembled from 1:1 GTP−tubulin complex (17 μM) in the presence of 2 molar equiv of taxol was measured using Optimas image analysis software from electron micrographs taken with a 35000-fold magnification.

the concentration of free P_i that has accumulated in the medium at the time of measurement. The enzyme-linked assay, in contrast, exhausts P_i from the medium as it is released. The fact that in the late stages of assembly more P_i appears bound to microtubules in the filter assay than in the enzyme-linked assay therefore suggests that more than one single microtubule−GDP−P_i intermediate may exist sequentially, in which P_i would display a gradually decreasing affinity for the site of the γ-phosphate of GTP. In this case, the lower-affinity P_i-bound species in equilibrium with free P_i would be detected in the filter assay, not in the enzyme-linked assay. More experiments are needed to test this hypothesis thoroughly.

The histogram of length distribution of microtubules assembled for 15 s from 17 μM tubulin and 34 μM taxol is shown in Figure 5. The average length was 0.21 μm. Microtubules therefore contained 350 subunits on average at the end of the rapid assembly process and grew from 0 to 0.21 μm within 15 s. This range of polymer length is smaller than the wavelength (350 nm) at which the turbidity measurements were made; hence, one cannot consider that the increase in turbidity is linearly correlated with the increase in polymer mass (Berne, 1974). In fact, in the early stages of the polymerization process, the specific increase in turbidity associated with the formation of very small sheets and short microtubules is lower than the specific turbidity change in the later steps of the polymerization reaction. Since a time-resolved analysis of the scattering properties of the different polymers during the assembly process is not available, the recorded time course of turbidity change cannot be corrected to represent the change in actual polymer mass; however, this correction would certainly yield a kinetic curve in which the half-time of assembly would be shorter that the measured half-time of the turbidity rise, which was 3 s. The value of the corresponding pseudo-first-order rate constant, 0.23 ± 0.04 s^{-1}, therefore is an underestimated value of k_+M, where M is the number concentration of microtubules, which equals 17000/350 = 49 nM. According to these numbers, the value of k_+ would be at least 0.23/0.049 = 4.7 μM^{-1} s^{-1}, in reasonable agreement with previously published values (Walker *et al.*, 1988; Mitchison & Kirschner, 1984). The maximum GTP + GDP−P_i cap size (reached at 6 s) was about 170−180 subunits. Assuming that the rate of GTP cleavage is a vectorial process with a single GDP−P_i−GTP boundary per microtubule, the value of 0.3 s^{-1} found for the apparent rate of cleavage would correspond to a rate of $0.3 \times 170 = 51$ s^{-1}, in satisfactory agreement with the value (30−40 s^{-1}) found in previous independent experiments (Carlier *et al.*, 1987b). If phosphate release is also assumed to proceed in a vectorial fashion, then the GDP−P_i−GDP boundary would migrate at a rate of $0.126 \times 170 = 21.4$ s^{-1} on each microtubule. The values found here for k_2 and k_3 are high enough to explain why the techniques used in previous works to evaluate the size of the GTP−GDP−P_i cap on growing microtubules (O'Brien *et al.*, 1987; Stewart *et al.*, 1990) which had a dead time of 10−20 s failed to detect a significant amount of these early intermediates. The rates measured for GTP hydrolysis and P_i release refer to tubulin polymers with taxol bound. These polymers exhibit an appreciable polymorphism with small open sheets coexisting with short closed microtubules. Despite the frequent opening of the polymers, which may be in relation with their small size, the lattice of taxol-induced tubulin polymers is of the microtubule type; hence, it is reasonable to think that the value found for the rate of P_i release applies to microtubules with taxol bound. We have no definite proof that the rate of P_i release is the same when taxol in not bound to microtubules.

ACKNOWLEDGMENT

We thank Dr. D. Pantaloni for helpful discussions and Dr. M. R. Webb for an initial gift of MESG and for communicating results (Webb, 1992) prior to publication.

REFERENCES

Berne, B. J. (1974) *J. Mol. Biol. 89*, 755−758.
Broom, A. D., & Robins, R. K. (1964) *J. Heterocycl. Chem. 1*, 113−114.
Burns, R. G. (1991) *Biochem. J. 277*, 231−238.
Caplow, M. (1986) *Ann. N. Y. Acad. Sci. 466*, 510−518.
Caplow, M., Shanks, J., & Ruhlen, R. L. (1988) *J. Biol. Chem. 263*, 10344−10352.

Caplow, M., Ruhlen, R. L., & Shanks, J. (1994) *J. Cell Biol. 127*, 779−788.
Carlier, M.-F. (1987) *Biochem. Biophys. Res. Commun. 143*, 1069−1075.
Carlier, M.-F. (1989) *Int. Rev. Cytol. 115*, 139−170.
Carlier, M.-F., & Pantaloni, D. (1981) *Biochemistry 20*, 1924−1932.
Carlier, M.-F., & Pantaloni, D. (1983) *Biochemistry 22*, 4814−4822.
Carlier, M.-F., & Pantaloni, D. (1988) *J. Biol. Chem. 263*, 817−825.
Carlier, M.-F., & Pantaloni, D. (1986) *Biochemistry 25*, 7789−7792.
Carlier, M.-F., Hill, T. L., & Chen, Y. (1984) *Proc. Natl. Acad.Sci. USA 81*, 772−776.
Carlier, M.-F., Melki, R., Pantaloni D., Hill, T. L., & Chen, Y. (1987a) *Proc. Natl. Acad. Sci. U.S.A. 84*, 5257−5261.
Carlier, M.-F., Didry, D., & Pantaloni, D. (1987b) *Biochemistry 26*, 4428−4437.
Carlier, M.-F., Didry, D., Melki, R., Chabre, M., & Pantaloni, D. (1988) *Biochemistry 27*, 3555−3559.
Detrich, H. W., III, & Williams, R. C. (1978) *Biochemistry 17*, 3900−3907.
Drechsel, D. N., & Kirschner, M. W. (1994) *Curr. Biol. 4*, 1053−1061.
Eisenberg, E., & Kielley, W. W. (1974) *J. Biol. Chem. 249*, 4742−4748.
Gordon, D. J., Yang, Y.-Z., & Korn, E. D. (1976) *J. Biol. Chem. 251*, 7474−7479.
Hill, T. L. (1985) *Proc. Natl. Acad. Sci. U.S.A. 82*, 431−435.
Hill, T. L. (1987) in *Linear Aggregation Theory in Biology* (Rich, A., Ed.) Springer-Verlag, New York.
Hill, T. L., & Carlier, M. F. (1983) *Proc. Natl. Acad. Sci. U.S.A. 80*, 7234−7238.
Horio, T., & Hotani, H. (1986) *Nature 321*, 605−607.
Hyman, A. A., Chretien, D., Arnal, I., & Wade, R. H. (1995) *J. Cell Biol. 128*, 117−125.
Krauhs, E., Little, M., Kempf, T., Hofer Warbinek, R., Ade, W., & Ponstingl, H. (1981) *Proc. Natl. Acad. Sci. U.S.A. 78*, 4156−4160.
McLean-Fletcher, S., & Pollard, T. D. (1980) *Biochem. Biophys. Res. Commun. 96*, 18−27.
Melki, R., & Carlier, M.-F. (1993) *Biochemistry 32*, 3405−3413.
Melki, R., Carlier, M.-F., Pantaloni, D., & Timasheff, S. N. (1989) *Biochemistry 28*, 9143−9152.
Melki, R., Carlier, M.-F., & Pantaloni, D. (1990) *Biochemistry 29*, 8921−8932.
Mitchison, T. J., & Kirschner, M. W. (1984) *Nature 312*, 237−242.
O'Brien, E. T., Voter, W. A., & Erickson, H. P. (1987) *Biochemistry 26*, 4148−4156.
Ohm, T., & Wegner, A. (1994) *Biochim. Biophys. Acta 1208*, 8−14.
Shelanski, M. L., Gaskin, F., & Cantor, C. R. (1973) *Proc. Natl. Acad. Sci. U.S.A. 70*, 765−768.
Spudich, J. A., & Watt, S. (1971) *J. Biol. Chem. 246*, 4866−4871.
Stewart, R. J., Farrell, K. W., & Wilson, L. (1990) *Biochemistry 29*, 6489−6498.
Trentham, D. R., Bradsley, R. G., Eccleston, J. F., & Weeds, A. G. (1972) *Biochem. J. 126*, 635−644.
Venier, P., Maggs, A. C., Carlier, M.-F., & Pantaloni, D. (1994) *J. Biol. Chem. 269*, 13353−13360.
Walker, R. A., O'Brien, E. T., Pryer, N. K., Sobeiro, M. F., Voter, W. A., Erickson, H. P., & Salmon, E. D. (1988) *J. Cell. Biol. 107*, 1437−1448.
Webb, M. R. (1992) *Proc. Natl. Acad. Sci. U.S.A. 89*, 4884−4887.
Weingarten, M. D., Lockwood, A. H., Hwo, S. Y., & Kirschner, M. W. (1975) *Proc. Natl. Acad. Sci. U.S.A. 72*, 1858−1862.

BI961325O